Strategies of model coupling: application to free surface flow problems

Edie Miglio Simona Perotto Fausto Saleri

MOX– Modellistica e Calcolo Scientifico
Dipartimento di Matematica "F. Brioschi"
Politecnico di Milano
via Bonardi 9, 20133 Milano, Italy
edie.miglio@mate.polimi.it, simona.perotto@mate.polimi.it,
fausto.saleri@mate.polimi.it

Abstract

The motion of water in a complex hydrodynamic configuration is characterized by a wide spectrum of space and time scales, due to the coexistence of physical phenomena of different nature. Consequently, the numerical simulation of a hydrodynamic system of this type is characterized by a large computational cost. In this paper, after introducing a quite general setting for model coupling, we discuss two techniques to reduce such a computational effort by suitably coupling different hydrodynamic models. The first approach is based on a dimensionally heterogeneous–physically homogeneous coupling strategy, driven by *a priori* physical considerations. As second strategy we suggest a dimensionally homogeneous–physically heterogeneous coupling. This time the "subdomain-to-model" correspondence is identified automatically thanks to a suitable *a posteriori* modeling error estimator. The range of applicability of both the approaches is finally examined on some test cases.

1 Introduction and motivations

Physical phenomena, taking place on large domains, are usually associated with the coexistence of heterogeneous physical features, often localized in specific portions of the domain. In view of a mathematical modeling of these phenomena, it is reasonable to resort to a model computationally cheap enough, but, at the same time, sufficiently accurate. It is obvious that a single model may not be adequate. Instead, a suitable model coupling approach seems more satisfactory, as it amounts to using simultaneously different mathematical models and solving the most complex ones only where it is strictly necessary, that is on restricted regions of the domain. As a meaningful example consider a typical aerodynamics problem: the simulation of the flow field around an airfoil where the equations for

compressible and incompressible fluids are merged. In more detail, the Navier-Stokes equations are solved in the boundary layer and in the downstream wake, the Euler equations in the surrounding region where the shock may develop, and the full potential equation in the far field where the flow is irrotational (see Section 8.3 in [1] and the references therein).

The heterogeneous nature of the physical phenomena suggests coupling heterogeneous mathematical models, supposed, for simplicity, only of non-overlapping type. In this framework we have essentially two different strategies:

1. *Dimensionally Homogeneous – Physically Heterogeneous Coupling.* Undoubtedly, this is the most straightforward and classical coupling. A reduction of the computational cost is guaranteed provided that the most complex model is solved on a reduced zone of the domain. To merge the models, suitable *matching conditions* are required. This turns out to be an easy or a hard task depending on the level of heterogeneity of of the involved models.

2. *Dimensionally Heterogeneous – Physically Homogeneous Coupling.* This technique allows us to considerably reduce the computational cost of the approximation procedure, especially if 1D models are involved in the coupling. Again, suitable *matching conditions*, this time relating dimensionally different quantities, are required.

Then both the strategies 1. and 2. can be performed according to the following paradigma:

A. *An a priori approach.* The regions of the domain where the different models have to be solved, are chosen only once, at the beginning of the approximation procedure. Usually, physical considerations drive such a choice and no computation is involved.
The static nature of the "subdomain-to-model" correspondence makes this technique particularly suitable for a computing parallelization. On the other hand, there exist many physical configurations where the choice of the zones where to use the different models is not immediate or feasible (see Section 2.4).

B. *An a posteriori approach.* The choice of the areas of the domain where to solve each model is made through an automatic tool. This can be achieved via a more rigorous mathematical analysis, for instance via a suitable modeling error estimator. Hence, using this approach, the a-priori physical analysis of the problem at hand (in order to decide the areas in which the more complex models have to be solved) can be avoided.
Two are the main drawbacks of this approach. First, the increase of the

computational cost related to the required a posteriori analysis. Then a computating parallelization is now less straightforward as the "subdomain-to-model" matchings change at each time. On the other hand, this last feature turns out to be favourable from a computational viewpoint, as the error estimator aims at minimizing, at each time, the portion of the domain where the more complex model has to be solved.

Overall, by suitably combining the strategies 1.-2., A.-B., we have four possible couplings.
The approach 1.-A. is strictly related to the domain decomposition theory and it is rather recurrent in the literature (see, e.g., [2, 3] and Sections 8.2 and 8.3 in [1]). On the other hand, the choice 2.-A. has been largely investigated in the haemodynamics framework (see [4, 5]).
The a posteriori analysis represents a very recent area of interest, and so far, essentially only the 1.-B. approach has been covered. The first works were related to the solid mechanics and to the elasticity theory (see, for instance, [6, 7, 8, 9]). In more recent developments, a burdensome analysis has led to a posteriori modeling error estimators also for steady Computational Fluid Dynamics (CFD) problems [10, 11]. Moreover, notice that, in the references above, only rather "nested" hierarchies of models have been employed. Namely, one model is obtained from the others simply by neglecting some terms.
From a computational viewpoint, it is evident that the most convenient approach is the 2.-B. strategy. However, this still represents an open-problem. To our knowledge, a first step in this direction is attempted in [12].

In this paper we provide an example of both the strategies 2.-A. and 1.-B. in the free surface flows framework, while highlighting further the range of applicability of the two approaches.

1.1 Coupling of hydrodynamic models

In the simulation of free surface flows a wide range of physical phenomena is involved: just consider tidal flows, water motion in lakes, large basins, river courses, channels, etc. Different space and time scales should be taken into account to capture all the physical features of the hydrodynamic problem at hand. Typically, the most suitable mathematical model is represented by the full 3D Navier-Stokes equations, whose computational cost is, however, excessively high. This is one of the reason why a large spectrum of simpler hydrodynamic models has been proposed in the literature (see, for instance, [13, 14, 15]).

By following the classifications 1. and 2. above, we distinguish between hydrodynamic models of different dimension (3D, 2D and 1D) and models derived under physical assumptions varying from one model to the other. According to the former classification, the most widespread three-dimensional models are the 3D free surface Navier-Stokes equations and the 3D hydrostatic shallow water system. Concerning the 2D case, the most popular models are the Saint-Venant, Serre and Boussinesq equations. Finally, the 1D counterparts of these

latter equations represent the simplest hydrodynamic models available in the literature. On the other hand, the physical classification split the hydrodynamic models into hydrostatic and non-hydrostatic models: the first category is essentially comprised of the Saint-Venant equations, while in the second class we find the Boussinesq and the Serre equations.

Now, moving from some standard hydrodynamic configurations, we particularize the general coupling approach above to the free surface flows framework, by providing an example for both the 2.-A. and the 1.-B. approaches, in Sections 2 and 3, respectively.

In Section 2 an a priori geometrical multiscale approach (which is a dimensional heterogeneous and physical homogeneous coupling) is tested by considering the motion of water along a river bifurcation. In more detail, we solve the 2D shallow water equations in correspondence of the bifurcation and a 1D Saint-Venant model after the bifurcation. This choice can be justified observing that the 2D features of the phenomenon should be more evident in the area around the bifurcation rather than along the straight branches of the river. Suitable matching conditions are provided for this coupling.
On the other hand, this a priori approach fails when studying a more complex hydrodynamic configuration, namely the motion of a solitary wave along a channel with an obstacle (see Section 2.4). In such a case an a priori "subdomain-to-model" matching turns out to be inadequate.

In Section 3 we suggest a different approach. A dynamic model adaptivity is suggested to improve the quality of the approximate solution. This is achieved via a suitable a posteriori modeling error estimator, i.e. thanks to a more rigorous mathematical analysis. Following a 1.-B. coupling strategy, we move from a hierarchy of 2D Saint-Venant like equations, thus providing a numerical tool able to automatically select the model of the hierarchy to be solved in the different portions of the domain. The results of a test case concerning the simulation of the motion of a soliton in a straight channel show the effectiveness of this approach: in particular no significant loose in the accuracy of the solution can be observed (see Section 3.4).

Finally, in Section 4, we sketch some possible future developments for this research. In particular a possible merge of the two approaches 1.-B. and 2.-A. is outlined.

2 An a priori geometrical multiscale approach

Let us consider the motion of water in a hydrodynamic system, where the vertical scales are much smaller compared with the corresponding horizontal ones. This feature allows us to exploit the shallow water theory, based on the hydrostatic approximation of the pressure, i.e., the pressure of the fluid is assumed to depend only on the total water depth only.
In the sequel, according to the coupling approach 2.-A., we merge the 2D with the

1D Saint-Venant equations. The main difficulty of such a technique is to find the proper matching conditions between the two models, as dimensionally different quantities have to be related. With this aim, we extend the approach provided in [16], where the 3D Navier-Stokes equations are coupled with a convenient 1D model for the description of blood flow in a compliant vessel, to the case of free surface flows. Though the dimension of the models is different, we resort to a similar analysis to derive the appropriate coupling conditions.

2.1 The coupled models

For the sake of simplicity we are going to consider a flat bottom channel with no friction effects. The 2D model is then represented by the Saint-Venant equations, with conservative form given by

$$\begin{cases} \dfrac{\partial(h\,\mathbf{u})}{\partial t} + \nabla\cdot(h\,\mathbf{u}\otimes\mathbf{u}) + g\,h\,\nabla h = \mathbf{0} & \text{with } (\mathbf{x},t)\in\mathcal{Q} \\ \dfrac{\partial h}{\partial t} + \nabla\cdot(h\,\mathbf{u}) = 0 & \text{with } (\mathbf{x},t)\in\mathcal{Q}, \end{cases} \tag{1}$$

where $\mathbf{u} = (u,v)^T$ is the average velocity, h denotes the total water depth, $\mathcal{Q} = \Omega\times(0,T]$ is the considered space-time domain, with Ω an open (regular) subset of $\mathbb{R}^2$, $T>0$ and $\mathbf{x} = (x,y)^T$. System (1) will be completed with suitable initial and boundary conditions to guarantee the well-posedness of the problem. In the sequel a sub-critical flow regimes will be assumed.

In some situations (for instance when 2D effects can be neglected), the hyperbolic system (1) is replaced by the 1D shallow water model, by assuming that the velocity is uniform over any cross section, that the channel is straight enough and its slope sufficiently mild and uniform throughout the region of interest. Moreover, the streamwise bottom slope and the lateral inflow are assumed equal to zero and the bottom friction is neglected as in the 2D case.

In the sequel, we focus on the case of one-dimensional channels with a constant rectangular cross-section. In such a case the 1D model reduces to the hyperbolic system

$$\begin{cases} \dfrac{\partial Q}{\partial t} + \dfrac{\partial}{\partial x}\left(\dfrac{Q^2}{A}\right) + gA\dfrac{\partial h}{\partial x} = 0 & \text{with } (x,t)\in\widetilde{\mathcal{Q}}, \\ \dfrac{\partial A}{\partial t} + \dfrac{\partial Q}{\partial x} = 0 & \text{with } (x,t)\in\widetilde{\mathcal{Q}}, \end{cases} \tag{2}$$

where A is the area of the wet cross-section, h the total water depth, $Q = Au$ the discharge, u being the average velocity, and $\widetilde{\mathcal{Q}} = (a,b)\times(0,T]$ the space-time domain under examination. It is understood that system (2) has to be supplied with proper initial and boundary conditions.

To find the coupling conditions between the 2D and the 1D shallow water models above, we have moved from the stability analysis of the two models. It is well known that the 2D system is stable under suitable initial and boundary

conditions and regularity assumptions (see, for instance, [17], or [18] for the viscous case).
Concerning the 1D system, we refer to [19] for a detailed a priori analysis, while itemizing here the corresponding main results.

It can be proved that the two real eigenvalues of the hyperbolic system (2) are given by $\lambda_{1,2} = u \pm c$, with $c(A) = \sqrt{gA/L}$ the celerity of the system, L being the width of the rectangular section. In such a case it is also possible to compute the characteristic variables

$$W_{1,2}(x,t) = u \pm \int_{A_0}^{A} \frac{c(\tau)}{\tau}\, d\tau = u \pm 2\sqrt{\frac{g}{L}}\,\left[\sqrt{A} - \sqrt{A_0}\right], \tag{3}$$

where A_0 is the area of the cross-section wetted by the constant undisturbed water of depth h_0. Moreover, we assume that, for any time $t \in (0,T]$, the area A remains strictly positive and that λ_1 and λ_2 have opposite sign ($\lambda_1 > 0$, $\lambda_2 < 0$). This is the same as considering a sub-critical and unidirectional flow, that is the most interesting situation in view of the coupling of (1) with (2).

We endow system (2) with the following general initial and boundary conditions:

$$A(x,0) = A^*(x), \quad Q(x,0) = Q^*(x) \quad \text{with} \quad a < x < b, \tag{4}$$

$$W_1(a,t) = g_1(t), \quad W_2(b,t) = g_2(t), \quad \text{with} \;\; t \in (0,T]. \tag{5}$$

Let us introduce the *energy* associated with model (2):

$$E(t) = \frac{1}{2g}\int_a^b A(x,t)\,u^2(x,t)\,dx + \frac{1}{2L}\int_a^b [A(x,t) - A_0]^2\,dx, \quad \text{with} \;\; t \in (0,T]. \tag{6}$$

The energy $E(t)$ turns out to be a positive function, for any $t \in (0,T]$ and for any A strictly positive.

The following conservation property can be proved:

Proposition 2.1 *For any $T > 0$, the equality*

$$E(T) + \int_0^T Q\Big((h - h_0) + \frac{1}{2\,g}\,u^2\Big)\Big|_a^b\, dt = E(0), \tag{7}$$

holds, $E(0)$ depending only on the initial values A^* and Q^*.

Result (7) can be used to derive an energy estimate for the 1D problem (2).

Proposition 2.2 *Let us assume that the boundary data g_1 and g_2 in* (5) *satisfy for any $t \in (0,T]$, the following restrictions*

$$g_1(t) > -2\sqrt{\frac{gA_0}{L}} \quad \textit{and} \quad g_2(t) < 2\sqrt{\frac{gA_0}{L}}\,. \tag{8}$$

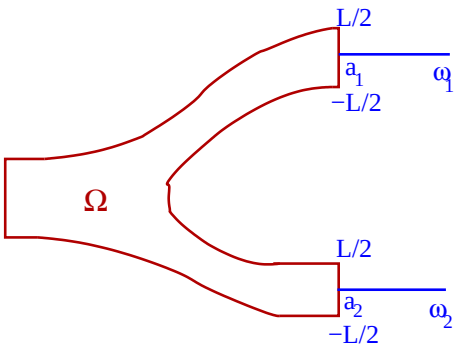

Figure 1: Sketch of a river bifurcation and the corresponding "subdomain-to-model" representation.

Then there exists a positive function $F = F\left(g_1, g_2, \dfrac{A_0}{L}\right)$ *such that*

$$E(T) \leq E(0) + \int_0^T F\left(g_1(t), g_2(t), \frac{A_0}{L}\right) dt\,, \tag{9}$$

i.e., the 1D model (2) *provided with conditions* (4)-(5) *is stable.*

Remark 2.1 *If homogeneous boundary conditions are chosen in* (5)*, estimate* (9) *simplifies to* $E(T) \leq E(0)$*, provided that* $2\sqrt{A_0}/3 < \sqrt{A} < 2\sqrt{A_0}$.

We point out also that, so far, no energy estimate is available in the literature in the presence of a general cross-section. However, stability results similar to (7) and (9) can be proved for one-dimensional channels with triangular and trapezoidal cross-section (see [20]).

2.2 The matching conditions

Let us consider the river bifurcation sketched in Figure 1, where Ω, ω_1 and ω_2 denotes the two-dimensional and 1D domains, respectively. The flow is assumed to go from left to right. Let $\mathbf{a}_k$, with $k = 1, 2$, be the *matching points* between Ω and ω_k, and let Γ_k denote the cross-sections of Ω at the points $\mathbf{a}_k$.
We assume that ω_1 and ω_2 represent two one-dimensional channels with rectangular cross-sections of the same width L and outward normals along the x-direction. In the subdomains ω_1 and ω_2, we solve the 1D shallow water model, thus yielding the physical quantities $A_{1\mathrm{D}}$, $Q_{1\mathrm{D}}$ and $h_{1\mathrm{D}}$ and, consequently, $u_{1\mathrm{D}} = Q_{1\mathrm{D}}/A_{1\mathrm{D}}$. At the left-hand side of $\mathbf{a}_1$ and $\mathbf{a}_2$, the 2D Saint-Venant equations are solved with associated physical quantities $A_{2\mathrm{D}}$, $Q_{2\mathrm{D}}$ and $h_{2\mathrm{D}}$.

The issue now consists of relating quantities of different dimension. Concerning the coupling 2D-1D, the reduction of the two-dimensional information to one-dimensional quantities is rather easy. We can, for instance, average the

2D terms along the cross-sections Γ_k, for $k = 1, 2$. With this aim, let us introduce the mean velocity, the mean total water depth and the mean discharge

$$\overline{u}_{2\mathrm{D}} = \frac{1}{L} \int_{-\frac{L}{2}}^{\frac{L}{2}} u(a,y)\, dy\,, \ \overline{h}_{2\mathrm{D}} = \frac{1}{L} \int_{-\frac{L}{2}}^{\frac{L}{2}} h(a,y)\, dy = \frac{A_{2\mathrm{D}}}{L}\,, \ \overline{Q}_{2\mathrm{D}} = A_{2\mathrm{D}}\, \overline{u}_{2\mathrm{D}}\,, \tag{10}$$

where $A_{2\mathrm{D}} = \int_{-\frac{L}{2}}^{\frac{L}{2}} h(a,y)\, dy$, u is the horizontal component of the 2D velocity $u_{2\mathrm{D}}$, and a coincides with the x-component of $\mathbf{a}_1$ or $\mathbf{a}_2$, respectively. Thanks to the unidirectional flow hypothesis, we have a subcritical outflow for the 2D system (with *two outgoing characteristics*) and a subcritical inflow for the one-dimensional problem (with *an incoming characteristic*). From a physical viewpoint it seems reasonable to demand the continuity of the following quantities at the interfaces $\mathbf{x} = \mathbf{a}_1$ and $\mathbf{x} = \mathbf{a}_2$:

i) the cross-section area: $A_{2\mathrm{D}} = A_{1\mathrm{D}}$, i.e. $A_{1\mathrm{D}} = \overline{h}_{2\mathrm{D}} L$;

ii) the discharge: $\overline{Q}_{2\mathrm{D}} = Q_{1\mathrm{D}}$;

iii) the entering characteristic: $2\,\overline{\sqrt{h_{2\mathrm{D}}\, g}} + \overline{u}_{2\mathrm{D}} = 2\,\sqrt{h_{1\mathrm{D}}\, g} + \dfrac{Q_{1\mathrm{D}}}{A_{1\mathrm{D}}}$.

Actually, notice that *ii)* is automatically guaranteed when *i)* and *iii)* hold.

2.3 The domain decomposition algorithm

A sub-domain iterative procedure is carried out to solve the coupled 2D-1D problem sketched in Figure 1. In more detail, three sub-problems are simultaneously solved on Ω, ω_1 and ω_2, while exchanging information one another through the cross-sections Γ_k, for $k = 1, 2$. Moving from the stability results cited in Section 2.1, we provide each sub-domain with suitable boundary conditions to guarantee the well-posedness of each sub-problem. In particular, at the matching points $\mathbf{a}_1$ and $\mathbf{a}_2$, we assign:

condition *i*) for imposing the total water depth at the *outflow* of the 2D model;

condition *iii*) at the *inflow* of the 1D model.

Concerning the remaining parts of the sub-domains boundary, we impose:

a) the total water depth $h(t)$ as a function of time at the *inflow* of the 2D model;

b) a non-reflecting boundary condition at the *outflow* of the 1D model;

c) no slip boundary conditions on the *rigid walls* of the river.

In more detail, given the solution of the coupled problem at time t^n, for $k = 1, 2, \ldots$ until convergence, let us

- solve the 2D problem provided with conditions *i*) and *a*), to obtain h_k^{n+1}, $\mathbf{u}_k^{n+1}$;
- compute $2\overline{\sqrt{h_k^{n+1}}\,g} + \overline{u}_k^{n+1}$, *i.e.* an approximation for the left-hand side of condition *iii*);
- solve the 1D problem completed with conditions *iii*) and *b*).

Notice that the notation q_k^{n+1} above, with $q = h$, $\mathbf{u}$, $\overline{u}$, is the valued yielded by the iterative procedure at the k-th step at the time t^{n+1}. The iterative nature of the algorithm above is justified with the aim of ensuring that the interface conditions above are satisfied within a fixed tolerance. We underline that, in practice, after 2 or 3 iterations, the difference between the 1D and the averaged 2D values is already very small. A more straightforward convergence analysis of the sub-domain iterative procedure above is going to be provided in a forthcoming paper.

Remark 2.2 *The matching and boundary conditions assigned above on each sub-domain are not the only ones possible. Alternative choices are currently under investigation.*

Remark 2.3 *If the reduction of higher dimensional quantities to corresponding lower ones is rather simple, the opposite process is less straightforward. Let us consider, for instance, a* 1D-2D *coupling. The simplest approach consists of assigning the same value along the whole* 2D *cross-section* Γ*, independently of the location of points in* Γ*. Obviously more sophisticated choices can be made, also taking into account the physical features of the phenomenon at hand.*

2.4 Numerical results

In this section we provide some numerical results to assess the effectiveness of the algorithm described in Section 2.

As for the discretization a space-time finite element scheme is adopted for both the 1D and the 2D model. In more detail we use the cG(1)dG(0) method *i.e.* a piecewise linear approximation in space and a piecewise constant (discontinuos) approximation in time [21, 22].

The first test case is concerned with the simulation of a river bifurcation, where a 2D model is employed in the area of the bifurcation and a 1D model is solved dowstream of the bifurcation itself (see Figure 1). At the inlet of the 2D model the following expression for the total depth is used:

$$\begin{cases} h(t) = 5 + 0.5 \sin\left(\dfrac{2\pi t}{10}\right), & t \leq 5, \\ h(t) = 5, & t > 5. \end{cases}$$

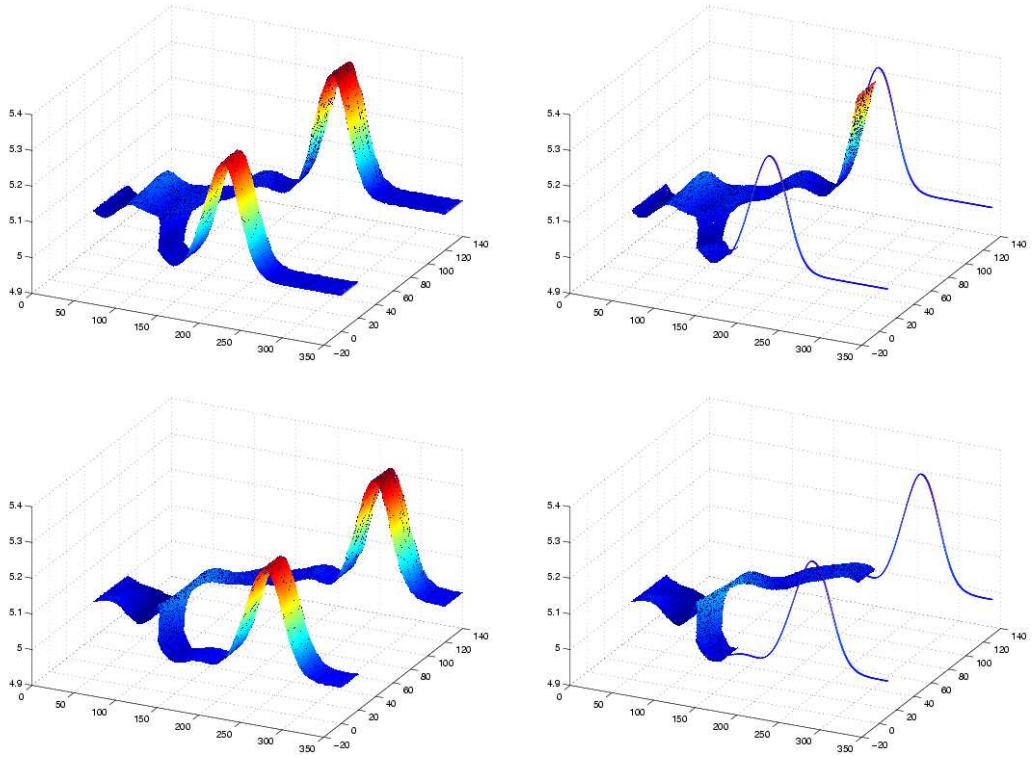

Figure 2: Comparison of the solution obtained at time $t = 250$ (top) and $t = 300s$ (bottom) using the full 2D model (left) and the coupled one (right).

The time step is set to $0.1s$, the total time of simulation is $300s$ and the mesh size is about $0.8m$.

Figure 2 shows a comparison between the results obtained using the full 2D model and the coupled 2D-1D model. It is worthwhile noticing that the wave amplitude, after the river bifurcation, provided by the coupled model is in good agreement with the results of the full 2D model. Moreover, also the reflected wave, due to the presence of the bifurcation, is correctly resolved by the coupled model. The second test case is aimed to evaluate the sensitivity of the results with respect to the extension of the zone where the 1D model is used. The motion of a solitary wave along a straight, channel $200m$ long and $20m$ wide, is simulated. The channel is characterized by the presence of a circular obstacle centered at $(x, y) = (30, 10)m$ with a radius $r = 4.5m$. Four different simulations have been carried out: in the first one a full 2D model is adopted on the whole domain; the other three simulations have been performed using the 2D model only for the first $100m$, $80m$ and $70m$, respectively. The initial condition for the

elevation and for the velocity are:

$$u(x,y,0) = \sqrt{11.76}\,\frac{0.2\mathrm{sech}^2(\sqrt{0.15}(x-10))}{5+0.2\mathrm{sech}^2(\sqrt{0.15}(x-10))}, \quad v(x,y,0)=0,$$

$$h(x,y,0) = 0.2\mathrm{sech}^2(\sqrt{0.15}(x-10))+5,$$

where the gravity g is taken equal to $1m/s^2$; the time step is $0.1s$ and we have used quasi uniform meshes with an average mesh parameter equal to $0.8m$.

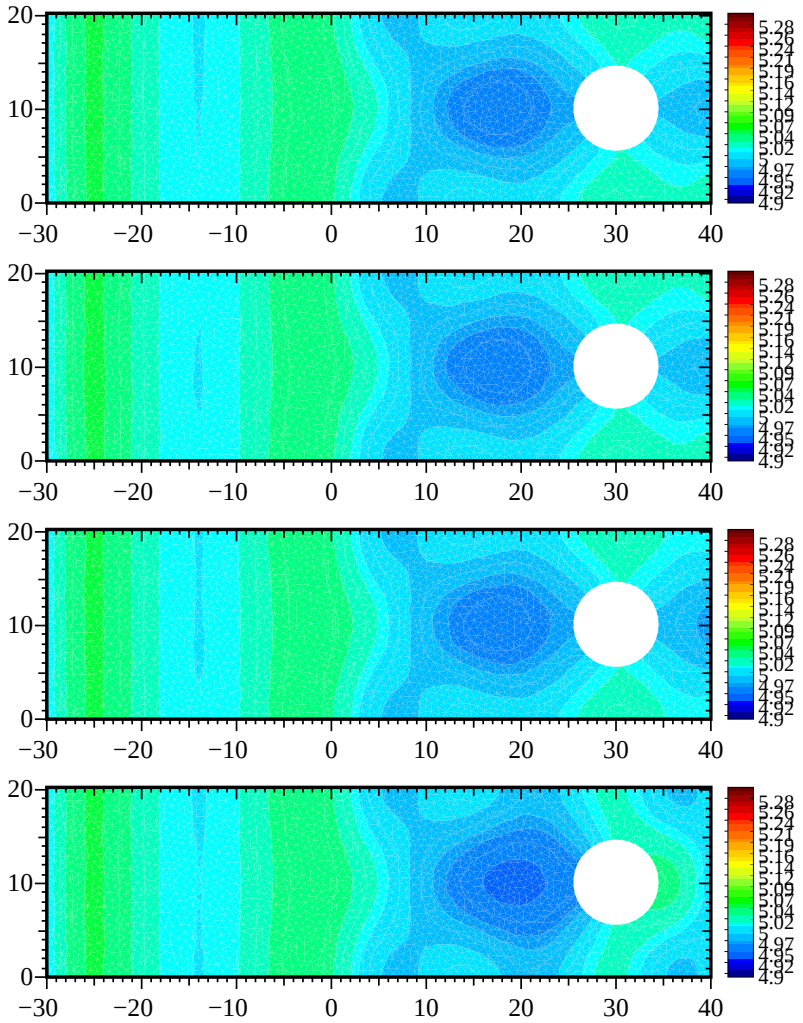

Figure 3: Elevations for the straight channel with an obstacle at $t = 14s$. From the top: full 2D model, 2D-1D coupled models where the 2D one is solved for $-30 \le x \le 70$, $-30 \le x \le 50$ and $-30 \le x \le 40$, respectively.

Figure 3 shows the results obtained using the full 2D model and the three different coupled 2D-1D models at $t = 14s$: only the first part of the domain

(namely for $x < 40m$) is shown. It can be noticed that the results of the coupled models are in good agreement with those obtained using the full 2D model provided that the junction between the 2D and the 1D model is sufficiently far away from the obstacle. This suggests that in this case an a priori "subdomain-to-model" assignement could yield a numerical not sufficiently accurate. Hence an automatic tool able to detect the zones where it is possible to solve the simpler model (without affecting the accuracy of the solution) would be very useful.

3 A posteriori model adaptivity for shallow water equations

The last test case of Section 2.4 is an example of a physical situation where the geometrical multiscale approach of Section 2 fails to provide a reliable numerical approximation. In such a case the dimensional reduction of the chosen physical model is not reasonable, probably due to strong 2D effects in the flow.

In this section we provide a different strategy to contain the computational cost of the numerical simulation without reducing its accuracy. The idea is to neglect, in some parts of the domain, some physical features of the phenomenon at hand (e.g., the nonlinear effects related to the convective terms), thus introducing a hierarchy of simplified models with the same space dimension. The issue is how to identify the areas of the domain where the full model or the simplified ones have to be solved. This matter will be tackled by deriving an a posteriori modeling error estimator, able to drive a suitable model adaption procedure.
We extend the analysis in [10] for steady equations to the case of unsteady free-surface flow problems. In more detail, a dual problem, associated with the problem at hand, is solved in order to measure the influence of the model on a user-defined output functional of the numerical solution. Standard examples of meaningful functionals in CFD are the lift and drag around bodies in external flows or mean and local values. In the framework of free surface flows we have considered, for instance, the kinetic energy and the vorticity of the flow [23]. This dual-based approach is ideal for a goal-oriented adaptivity and it generalizes to modeling error analysis the well-known *dual-weighted residual* method provided in [24] for the a posteriori discretization error control.

3.1 The coupled models

Let us consider the hierarchy of free-surface flow models:

$$\begin{cases} \dfrac{\partial \mathbf{u}_\alpha}{\partial t} + \alpha\,(\mathbf{u}_\alpha \cdot \nabla)\mathbf{u}_\alpha + g\,\nabla h_\alpha = 0 & \text{with } \ (\mathbf{x},t) \in \mathcal{Q}, \\ \dfrac{\partial h_\alpha}{\partial t} + \nabla \cdot (h_\alpha \mathbf{u}_\alpha) = 0 & \text{with } \ (\mathbf{x},t) \in \mathcal{Q}, \end{cases} \tag{11}$$

where $\mathbf{u}_\alpha(0) = \mathbf{u}_0^\alpha$, $h_\alpha(0) = h_0^\alpha$, $\mathbf{u}_0^\alpha$ and h_0^α being the initial data, and $\alpha = \alpha(\mathbf{x}, t) \in L^\infty(\mathcal{Q})$ is a piecewise constant function. In general we have $0 \leq \alpha \leq 1$, but throughout we suppose that α assumes only the values 0 and 1. At each time t^n, the nonlinear convective term in the momentum equation will be "switched-on" in the regions of Ω where $\alpha(\mathbf{x}, t^n) = 1$, ideally only where the nonlinear features of the problem at hand will be dominant. The unknowns $\mathbf{u}_\alpha$ and h_α preserve the same meaning as in (1). Moreover, proper boundary conditions will be supplied to the hyperbolic system (11), depending on the considered hydrodynamic problem. In the sequel we will refer to (11) as to the *adapted model*.

The choice $\alpha = 1$, for any $(\mathbf{x}, t) \in \mathcal{Q}$, provides us with the *fine* model, that is with the Saint-Venant equations (1), written in the non-conservative form:

$$\begin{cases} \dfrac{\partial \mathbf{u}_1}{\partial t} + (\mathbf{u}_1 \cdot \nabla)\mathbf{u}_1 + g\,\nabla h_1 = 0 & \text{with } \ (\mathbf{x}, t) \in \mathcal{Q}, \\ \dfrac{\partial h_1}{\partial t} + \nabla \cdot (h_1 \mathbf{u}_1) = 0 & \text{with } \ (\mathbf{x}, t) \in \mathcal{Q}, \end{cases} \tag{12}$$

with $\mathbf{u}_1(0) = \mathbf{u}_0^1$, $h_1(0) = h_0^1$ the initial data. Notice that, from a computational viewpoint, system (12) is the most expensive one. The expectation is to never solve the fine model on the whole domain, but only on a reduced portion of Ω.

On the other hand, if α is identically equal to zero in $\mathcal{Q}$, the adapted problem reduces to the *coarse problem*

$$\begin{cases} \dfrac{\partial \mathbf{u}_0}{\partial t} + g\,\nabla h_0 = 0 & \text{with } \ (\mathbf{x}, t) \in \mathcal{Q}, \\ \dfrac{\partial h_0}{\partial t} + \nabla \cdot (h_0 \mathbf{u}_0) = 0 & \text{with } \ (\mathbf{x}, t) \in \mathcal{Q}. \end{cases} \tag{13}$$

Typically, problem (13) will be never solved on the whole Ω. Were this the case, it could mean that the hydrodynamics involved in the problem at hand is simpler than what expected a priori, and the coarse model would suffice to reasonably describe the phenomenon.

To summarize, at each time t^n, neither the fine problem (12) nor the coarse one (13) will be solved on whole Ω. The discretized problem will be the adapted model (11), according to the value of $\alpha(\mathbf{x}, t^n)$.

To shorten the notations, we introduce in the sequel the "global" unknown $U_\alpha = (\mathbf{u}_\alpha, h_\alpha)$.

3.2 A modeling error estimator for the shallow water equations

Let $\mathcal{F}$ be the output functional we are interested in, possibly nonlinear. We aim to identify the regions of the domain where the two models (12) and (13) have to be solved, so that the quantity $\mathcal{F}(U_1) - \mathcal{F}(U_\alpha)$, at $t = T$, be below a prescribed tolerance, while minimizing the computational cost. Such a task is achieved via

a suitable a posteriori modeling error analysis, i.e. by controlling $\mathcal{F}(U_1)-\mathcal{F}(U_\alpha)$ in terms of the adapted quantity U_α.

With this aim, let us consider the weak form associated with the fine problem (12) which reads as: find $U_1 \in \mathcal{W} \equiv \mathcal{V} \times \mathcal{Z}$ such that, for any test function pair $\Psi = (\mathbf{v},\, q) \in \mathcal{W}$,

$$\Big(\frac{\partial U_1}{\partial t},\, \Psi\Big) + a(U_1)(\Psi) + d(U_1)(\Psi) = 0, \tag{14}$$

with $U_1(0) = U_0^1 = (\mathbf{u}_0^1, h_0^1)$ the initial data vector, and where

$$\Big(\frac{\partial U_1}{\partial t},\, \Psi\Big) = \Big(\frac{\partial \mathbf{u}_1}{\partial t},\, \mathbf{v}\Big) + \Big(\frac{\partial h_1}{\partial t},\, q\Big) \tag{15}$$

and

$$a(U_1)(\Psi) = g\ (\nabla h_1,\, \mathbf{v}) + \big(\nabla\cdot(h_1\mathbf{u}_1),\, q\big), \qquad d(U_1)(\Psi) = \big((\mathbf{u}_1\cdot\nabla)\mathbf{u}_1,\, \mathbf{v}\big) \tag{16}$$

are semilinear forms, linear with respect to Ψ but nonlinear in U_1. Concerning the choice of the functional spaces $\mathcal{V}$ and $\mathcal{Z}$, they will be proper subspaces of $[H^1(\Omega)]^2$ and $H^1(\Omega)$, respectively, suitably taking into account the boundary conditions completing system (12); we refer to [25] for the defintion of the Sobolev space $H^1(\Omega)$.
We assume that the solution U_1 of (14) exists unique in $\mathcal{W}$. This hypothesis allows us to write problem (14) as a constrained minimization problem, according to an optimal control approach: find $U_1 \in \mathcal{W}$ such that

$$\mathcal{F}(U_1) = \inf_{v\in M} \mathcal{F}(v), \tag{17}$$

with

$$M = \Big\{ v \in \mathcal{W} \ :\ \Big(\frac{\partial v}{\partial t}, \xi\Big) + a(v)(\xi) + d(v)(\xi) = 0,\ \text{for any } \xi \in \mathcal{W}\Big\}, \tag{18}$$

$\mathcal{F}(\cdot)$ being the chosen goal output functional. The minimum U_1 of (17) coincides with the first component of the saddle point $\widetilde{x}_1 = (U_1, Z_1) \in \widetilde{X} = [\mathcal{W}]^2$ of the *fine* Lagrangian

$$L(\widetilde{x}_1) = \mathcal{F}(U_1) - a(U_1)(Z_1) - d(U_1)(Z_1) - \Big(\frac{\partial U_1}{\partial t},\, Z_1\Big), \tag{19}$$

$Z_1 = (\mathbf{w}_1, \kappa_1) \in \mathcal{W}$ being the Lagrange multipliers (or influence functions) associated with the functional $\mathcal{F}(\cdot)$. The critical points $\widetilde{x}_1$ of $L(\cdot)$ are such that, for any test-functions pair $y = (\Phi, \Psi) \in \widetilde{X}$,

$$L'(\widetilde{x}_1)(y) = 0, \tag{20}$$

where

$$\begin{aligned} L'(\widetilde{x}_1)(y) \ &= \ \mathcal{F}'(U_1)(\Phi) - a'(U_1)(\Phi, Z_1) - d'(U_1)(\Phi, Z_1) - \Big(\frac{\partial \Phi}{\partial t}, Z_1\Big) \\ &- \ a(U_1)(\Psi) - d(U_1)(\Psi) - \Big(\frac{\partial U_1}{\partial t}, \Psi\Big) \end{aligned} \tag{21}$$

denotes the derivative of $L(\cdot)$ applied to the test function y, and $\Phi = (\boldsymbol{\varphi}, \vartheta) \in \mathcal{W}$. The derivatives in (21) are Gâteaux derivatives, $L(\cdot)$ being a differentiable functional on $\widetilde{X}$. In more detail, we have that the semilinear forms

$$a'(U_1)(\Phi, Z_1) = g(\nabla\vartheta, \mathbf{w}_1) + \big(\nabla\cdot(h_1\boldsymbol{\varphi}), \kappa_1\big) + \big(\nabla\cdot(\vartheta\mathbf{u}_1), \kappa_1\big), \tag{22}$$

$$d'(U_1)(\Phi, Z_1) = \big((\mathbf{u}_1\cdot\nabla)\boldsymbol{\varphi}, \mathbf{w}_1\big) + \big((\boldsymbol{\varphi}\cdot\nabla)\mathbf{u}_1, \mathbf{w}_1\big), \tag{23}$$

preserve the nonlinearity in U_1 but are linear in Φ and Z_1, while the definition of $\mathcal{F}'(U_1)(\Phi)$ depends on the chosen goal functional $\mathcal{F}$.
Thanks to (20), the minimization problem (17) is equivalent to solving the primal fine problem (14) together with the corresponding dual one: find $Z_1 \in \mathcal{W}$ such that, for any test function pair $\Phi \in \mathcal{W}$,

$$\Big(\frac{\partial\Phi}{\partial t},\, Z_1\Big) + a'(U_1)(\Phi, Z_1) + d'(U_1)(\Phi, Z_1) = \mathcal{F}'(U_1)(\Phi), \tag{24}$$

with $Z_1(T) = Z_T^1 = (\mathbf{w}_T^1, \kappa_T^1)$ the final data vector. Notice the linearity of the dual problem with respect to the influence function Z_1.

Now, let us consider the adapted model (11), whose corresponding weak form reads as: find $U_\alpha \in \mathcal{W}$ such that, for any $\Psi = (\mathbf{v},\, q) \in \mathcal{W}$,

$$\Big(\frac{\partial U_\alpha}{\partial t},\, \Psi\Big) + a(U_\alpha)(\Psi) + d(U_\alpha)(\alpha\Psi) = 0, \tag{25}$$

with $U_\alpha(0) = U_0^\alpha = (\mathbf{u}_0^\alpha, h_0^\alpha)$, and where the scalar product $(\partial U_\alpha/\partial t,\, \Psi)$ and the semilinear forms $a(U_\alpha)(\cdot)$ and $d(U_\alpha)(\cdot)$ are defined as in (15) and (16), respectively.

Let us repeat the minimization procedure used on the fine model (12). Thus we are led to find the critical points $\widetilde{x}_\alpha = (U_\alpha, Z_\alpha) \in \widetilde{X}$ of the *adapted* Lagrangian

$$L_\alpha(\widetilde{x}_\alpha) = \mathcal{F}(U_\alpha) - a(U_\alpha)(Z_\alpha) - d(U_\alpha)(\alpha Z_\alpha) - \Big(\frac{\partial U_\alpha}{\partial t},\, Z_\alpha\Big), \tag{26}$$

i.e., to look for the solution $U_\alpha \in \mathcal{W}$ of the primal adapted problem (25), and the solution $Z_\alpha = (\mathbf{w}_\alpha, \kappa_\alpha) \in \mathcal{W}$ of the associated dual problem: find $Z_\alpha \in \mathcal{W}$ such that, for any $\Phi \in \mathcal{W}$,

$$\Big(\frac{\partial\Phi}{\partial t},\, Z_\alpha\Big) + a'(U_\alpha)(\Phi, Z_\alpha) + d'(U_\alpha)(\Phi, \alpha Z_\alpha) = \mathcal{F}'(U_\alpha)(\Phi), \tag{27}$$

with $Z_\alpha(T) = Z_T^\alpha = (\mathbf{w}_T^\alpha, \kappa_T^\alpha)$, and where the semilinear forms $a'(U_\alpha)(\cdot,\cdot)$ and $d'(U_\alpha)(\cdot,\cdot)$ are defined as in (22) and (23), respectively.

To provide the desired modeling error estimator for the shallow water equations, let us introduce the following *modeling residuals*:

$$\rho_M(U_\alpha)(Z_\alpha) = -d(U_\alpha)\big((1-\alpha)Z_\alpha\big) = -\big((\mathbf{u}_\alpha\cdot\nabla)\mathbf{u}_\alpha,\, (1-\alpha)\mathbf{w}_\alpha\big), \tag{28}$$

$$\rho_M(U_\alpha)(E_Z) = -d(U_\alpha)\big((1-\alpha)E_Z\big) = -\big((\mathbf{u}_\alpha\cdot\nabla)\mathbf{u}_\alpha,\,(1-\alpha)(\mathbf{w}_1-\mathbf{w}_\alpha)\big), \quad (29)$$

$$\begin{aligned}\overline{\rho}_M(U_\alpha)(E_U,Z_\alpha) &= -d'(U_\alpha)\big(E_U,(1-\alpha)Z_\alpha\big)\\ &= -\big((\mathbf{u}_\alpha\cdot\nabla)(\mathbf{u}_1-\mathbf{u}_\alpha),(1-\alpha)\mathbf{w}_\alpha\big)\\ &- \big(\big((\mathbf{u}_1-\mathbf{u}_\alpha)\cdot\nabla\big)\mathbf{u}_\alpha,(1-\alpha)\mathbf{w}_\alpha\big), \quad (30)\end{aligned}$$

where $E_U = (\mathbf{u}_1-\mathbf{u}_\alpha, h_1-h_\alpha)$ and $E_Z = (\mathbf{w}_1-\mathbf{w}_\alpha, \kappa_1-\kappa_\alpha)$ are the primal and dual error, respectively. The residuals $\rho_M(U_\alpha)(\cdot)$ and $\overline{\rho}_M(U_\alpha)(\cdot,Z_\alpha)$ measure the extent to which the adapted solutions (U_α, Z_α) fail to satisfy the fine problems (14) and (24), respectively.

We are now in a position to state the main result of this section, while referring to [23] for the corresponding proof.

Proposition 3.1 *If the semilinear forms $a(U_1)(\cdot)$ and $d(U_1)(\cdot)$ defined in* (16) *and the functional $\mathcal{F}(U_1)$ are sufficiently differentiable with respect to U_1, then it holds that*

$$\mathcal{F}(U_1)-\mathcal{F}(U_\alpha) = \rho_M(U_\alpha)(Z_\alpha) + \frac{1}{2}\big\{\rho_M(U_\alpha)(E_Z) + \overline{\rho}_M(U_\alpha)(E_U,Z_\alpha)\big\} + R(\widetilde{x}_\alpha)\ , \quad (31)$$

where the residuals are defined as in (28),(29) *and* (30)*, while $R(\widetilde{x}_\alpha)$ is a remainder term.*

According to [23], to get computationally useful information from (31), we make some simplifying hypotheses on $L'(x)(\cdot)$ and on the semilinear form $d(U)(\cdot)$. We assume that there exists a constant $\gamma > 0$ such that, for any x_n and $x_m \in \widetilde{X}$,

$$\|x_n - x_m\|_{\widetilde{X}} \le \gamma\, \|L'(x_n) - L'(x_m)\|_{\widetilde{X}'}, \quad (32)$$

where $\|\cdot\|_{\widetilde{X}}$ and $\|\cdot\|_{\widetilde{X}'}$ are the norms associated with the space $\widetilde{X}$ and its dual $\widetilde{X}'$, respectively. Moreover, $d(U)(\cdot)$ and its derivatives are assumed sufficiently small, for any $U \in \mathcal{W}$.
Thus, the right-hand side of (31) reduces to the desired a posteriori modeling error estimator η_α for the goal quantity $\mathcal{F}(U_1) - \mathcal{F}(U_\alpha)$:

$$\mathcal{F}(U_1) - \mathcal{F}(U_\alpha) \simeq \eta_\alpha = \rho_M(U_\alpha)(Z_\alpha). \quad (33)$$

3.3 The algorithm

Let us sketch the algorithm for choosing which model of the hierarchy (11) has to be solved at each time on each mesh element K, to guarantee a prescribed tolerance τ on the error functional $\mathcal{F}(U_1) - \mathcal{F}(U_\alpha)$ at $t = T$. Let us introduce a fixed space-time partition consisting of N_h elements and N_t time intervals. To start the model adaption procedure we need to have a reference primal and dual solution. With this aim, we first solve the coarse primal problem (13) on $(0,T]$, together with the corresponding dual problem (namely equation (27) with $\alpha = 0$) on $(T,0]$. Thus we are in a position to apply the adaptive procedure below:

1) via a suitable *localization* procedure, the estimator η_α in (33) is evaluated on every $K \in \mathcal{T}_h$, thus yielding the local modeling error estimator $\eta_{\alpha,K} = \eta_\alpha|_K$;

2) then:

   a) if $\eta_{\alpha,K} \leq \dfrac{\tau}{N_h N_t}$, then $\alpha|_K = 0$, i.e. the piecewise constant function α in (11) is chosen equal to 0 on the triangle K;

   b) if $\eta_{\alpha,K} > \dfrac{\tau}{N_h N_t}$, then $\alpha|_K = 1$, i.e. the piecewise constant function α in (11) is chosen equal to 1 on the triangle K.

Notice that a sub-iteration on the points 2)-a) and 2)-b) will be likely required to guarantee the global quantity $\mathcal{F}(U_1) - \mathcal{F}(U_\alpha)$ to be really under the tolerance τ at $t = T$, in spite of the localization procedure. Moreover the check at the points 2)-a) and 2)-b) entails a space-time equidistribution criterion of the modeling error on the elements of the mesh $\mathcal{T}_h$.

3.4 Numerical results

In this section we are going to consider again the second test case presented in Section 2.4. The discretization scheme and the parameters of the simulation are the same.

The aim is to identify, at each time step, which are the areas of the domain where the fine model has to be solved in order to keep the quantity $\mathcal{F}(U_1) - \mathcal{F}(U_\alpha)$ at $t = T$, less than a give tolerance τ. We have considered the following goal-functional $\mathcal{F}(U) = \int_0^T \int_\Omega |U|^2 \, d\Omega \, dt$.

First of all let us consider the evolution in time of the kinetic energy for the fine, the coarse and the adapted models (see Figure 4, on the left). It can be noticed that for $\tau = 10^{-3}$ the curves of the adapated and of the fine model are almost coincident. Moreover by means of the adaptive procedure of Section 3 the number of elements where the fine model is solved is small compared to the total number of triangles of the mesh (see Figure 4, on the right)

Finally figure 5 shows the evolution of the areas where the fine model has to be solved for a tolerance $\tau = 10^{-3}$.

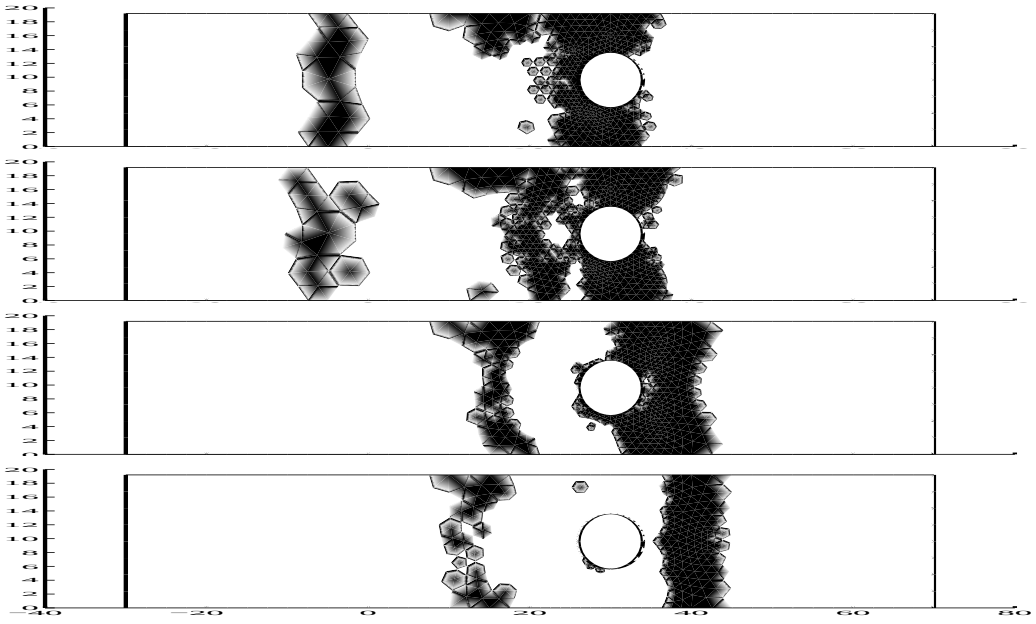

Figure 5: Four snapshots of the areas (in black) where α is equal to 1: from the top to the bottom at times $t = 8s, 10s, 12s$ and $14s$.

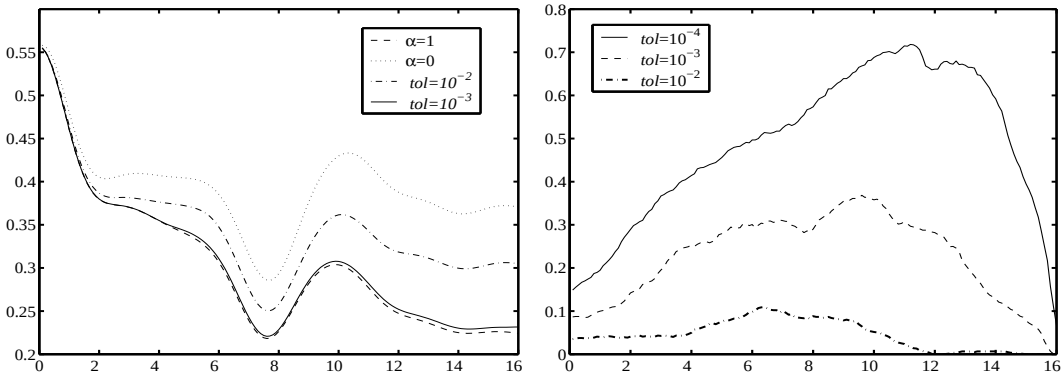

Figure 4: On the left the evolution in time of the kinetic energies of the coarse ($\alpha = 0$), the fine ($\alpha = 1$) and the adapted models (with two different tolerance τ). On the right the evolution in time of the fraction of the elements of the mesh where the fine model is solved for three different values of the tolerance τ.

4 Conclusions and...a look ahead

In this paper we propose two possible techniques to reduce the computational effort associated with the simulation of a complex hydrodynamic configuration.

The leading idea is to suitably couple hydrodynamic models, different from a physically and/or a dimensionally viewpoint. In more detail, the first approach is based on an a priori dimensionally heterogeneous–physically homogeneous coupling strategy, while the second one moves from an a posteriori dimensionally homogeneous–physically heterogeneous coupling. The reference hydrodynamic models are the standard Saint-Venant equations.
According to the numerical results in Sections 2.4 and 3.4, we argue that if the considered hydrodynamic configuration is simple (e.g., a straight channel or a river bifurcation), then the a priori approach can suffice to get satisfactory results. Otherwise, in the presence of a slightly more complex configuration (for instance, a channel with an obstacle) the a priori strategy fails, unless the region of the domain where the computationally cheaper model is solved, is very limited. In such a case, the a posteriori approach seems to be more convenient. The rigorous mathematical analysis driving the a posteriori strategy, provides us with a more expensive but robust numerical tool.
From these considerations, we ansatz that the more convenient strategy could be an a posteriori dimensionally heterogeneous–physically homogeneous coupling. This approach is still rather unexplored in the literature ([12]). in a forthcoming paper we will investigate this idea and try to make the two approaches described in this paper mutually "feeding".

Acknowledgments

We would like to thanks Dr. S. Micheletti and Prof. A. Veneziani for the fruitful discussion and for the useful suggestions they gave us during the preparation of this paper.

References

[1] A. Quarteroni and A. Valli, *Domain decomposition methods for partial differential equations*, Oxford University Press Inc., New York, 1999.

[2] L. Fatone, P. Gervasio and A. Quarteroni, *Multimodels for incompressible flows: iterative solutions for the Navier-Stokes/Oseen coupling*, M2AN Math. Model. Numer. Anal., 35 (2001), pp. 549–574.

[3] A. Quarteroni and L. Stolcis, *Heterogeneous domain decomposition for compressible flows*, in Proceedings of the ICFD Conference on Numerical Methods for Fluid Dynamics, M. Baines and W.K. Morton, Eds., Oxford University Press, Oxford, 1995, pp. 113-128.

[4] L. Formaggia and A. Quarteroni, *Mathematical Modelling and Numerical Simulation of the Cardiovascular System*, in Modelling of Living Systems,

Handbook of Numerical Analysis, N. Ayache, P.G. Ciarlet, J.L. Lions, Eds., Elsevier Science, Amsterdam, to appear.

[5] L. Formaggia, F. Nobile, A. Quarteroni and A. Veneziani, *Multiscale modelling of the circolatory system: a preliminary analysis*, Comput. Visual. Sci., 2 (1999), pp. 75-83.

[6] R.L. Actis, B.A. Szabo and C. Schwab, *Hierarchic models for laminated plates and shells*, Comput. Methods Appl. Mech. Engrg., 172 (1999), pp. 79–107.

[7] J.T. Oden, and K.S. Vemaganti, *Estimation of local modeling error and goal-oriented adaptive modeling of heterogeneous materials. I. Error estimates and adaptive algorithms*, J. Comput. Phys., 164 No. 1 (2000), pp. 22–47.

[8] J.T. Oden, and K.S. Vemaganti, *Estimation of local modeling error and goal-oriented adaptive modeling of heterogeneous materials. II. A computational environment for adaptive modeling of heterogeneous elastic solids*, Comput. Methods Appl. Mech. Engrg., 190 No. 46-47 (2001), pp. 6089–6124.

[9] E. Stein, and S. Ohnimus, *Anisotropic discretization- and model-error estimation in solid mechanics by local Neumann problems*, Comput. Methods Appl. Mech. Engrg., 176 (1999), pp. 363–385.

[10] M. Braack, and A. Ern, *A posteriori control of modeling errors and discretizatin errors*, Multiscale Model Simul., 1 No.2 (2003), pp. 221–238.

[11] J.T. Oden, and S. Prudhomme, *Estimation of modeling error in computational mechanics*, J. Comput. Phys., 182 (2002), pp. 469–515.

[12] M. Amara, D. Capatina-Papaghiuc and D. Trujillo, *Hydrodynamical modelling and multidimensional approximation of estuarian river flows*, Comput. Visual. Sci., 6 (2004), pp. 39-46.

[13] J.J. Stoker, *Water Waves, the Mathematical Theory with Applications*, Wiley, New York, 1958.

[14] C.B. Vreugdenhil, *Numerical Methods for Shallow-Water Flows*, Kluwer Academic Press, Dordrecht, 1998.

[15] G.B. Whitham, *Linear and Nonlinear Waves*, John Wiley & Sons Inc., New York, 1999.

[16] L. Formaggia, J.F. Gerbeau, F. Nobile, and A. Quarteroni, *On the coupling of 3D and 1D Navier-Stokes equations for flow problems in compliant vessels*, Comput. Methods Appl. Mech. Engrg., 191 (2001), pp. 561–582.

[17] P.L. Lions, *Mathematical Topics in Fluid Mechanics- Compressible Models*, Oxford Lecture Series in Mathematics and Its Applications, Vol. 2, No. 10. Oxford University Press, 1998.

[18] V.I. Agoshkov, D. Ambrosi, V. Pennati, A. Quarteroni and F. Saleri, *Mathematical and numerical modelling of shallow water flow*, Comput. Mech., 11, (1993), pp. 280–299.

[19] E. Miglio, S. Perotto, and F. Saleri, *A multiphysics strategy for free surface flows*, accepted for the publication in *Lecture Notes in Computational Sciences and Engineering*, Proceedings of the 15th International Conference on Domain Decomposition Methods, R. Kornhuber, R.H.W. Hoppe, D.E. Keyes, J. Periaux, O. Pironneau, J. Xu, Eds., Springer-Verlag (2003).

[20] M. Miglio, S. Perotto, and F. Saleri, *On the coupling of 2D and 1D shallow water models for the simulation of free surface flows*, in preparation.

[21] V. Girault, and P.A. Raviart, *Finite Element Methods for Navier-Stokes Equations: Theory and Algorithms*, Springer Series in Computational Mathematics, Vol. 5, Springer-Verlag, Berlin, 1986.

[22] K. Eriksson, D. Estep, P. Hansbo and C. Johnson, *Computational Differential Equations*, Cambridge University Press, Cambridge, 1996.

[23] M. Miglio, S. Perotto, and F. Saleri, *Adaptive modeling for free surface flows*, submitted for the publication in M2AN Math. Model. Numer. Anal. (2004).

[24] R. Becker, and R. Rannacher, *An optimal control approach to a posteriori error estimation in finite element methods*, in Acta Numerica 2001, A. Iserles, ed., Cambridge University Press, Cambridge, UK, 2001.

[25] J.L. Lions, and E. Magenes, *Non-Homogeneous Boundary Value Problems and Applications*, Volume I. Springer-Verlag, Berlin, 1972.